NUMERICAL PREDICTION OF EROSION WEAR FOR HYDRAULIC SPOOL VALVE

Jiayang YUAN*, Yaobao YIN*, Shengrong GUO**

*College of Mechanical Engineering, Tongji University
4800 CaoAn Road, Shanghai, 201804 China
(E-mail: jiayangyuan2010@163.com)
**Aviation Key Laboratory of Science and Technology on Aero Electromechanical System Integration, Nanjing Mechatronic and Hydraulic Engineering Research Centre, Nanjing, China

Abstract. The flow characteristics of hydraulic spool valve change significantly due to the solid particle erosion. In the present work, a numerical mechanism model is established to predict the material removal rate and the worn profile with erosion. First, Reynolds stress model is used to obtain the fluid phase information. Second, the particle trajectory is solved by a stochastic separated flow model. Third, an erosion formula is selected to calculate the local erosion rate. Then, a time-discrete and spatial-discrete update method is proposed to obtain the worn profile. The worn profiles obtained by model accord well with experiments, and, the shape of the worn profile is not quarter-circle, the quarter-circle assumption that always used in the erosion prediction of spool valve can lead to the erroneous result. By comparing with the laboratory experiments and a field case, the present model is well verified.

Keywords: hydraulic, erosion wear, sliding spool valve, numerical prediction, worn profile

INTRODUCTION

Spool valve is a type of principal control component in hydraulic systems, and always used as the power output stage of servo valve (shown in FIGURE 1) which is widely used in aviation, aerospace, ship and other modern major equipment areas. In spool valve, the fluid flows between a pair of sharp edges, and the solid particles that carried by the fluid impact the target surface with high velocity, leads to the erosion wear. The metering edges will become blunt and the lap of spool and bushing will decrease due to the solid particle erosion. Then, the spool valve null region characteristics that have an important influence on the system correct operation and stability will be degraded. So the erosion prediction of spool valve is important to the reliability evaluation and life-cycle performance prediction of hydraulic servo system.

The erosion in turbine [1], pump casing [2], pipes [3] and various valves [4] are studied theoretically. Most of the investigators focus on the wear location and the initial erosion rate to obtain the erosion protection scheme, but the worn profile prediction always be ignored. For spool valve, the worn profile of metering edges must be concerned, because the null behaviors are sensitive to the shape of metering edge. In some theoretical studies [5], the shape of worn metering edge is always simply assumed as quarter-circle without proof. But the erosion experiments of spool valve by Vaughan [6] show a different worn profile and indicate that the erosion prediction may be incorrect under the quarter-circle assumption. So, in addition to erosion rate, the prediction of worn profile based on the mechanism model is necessary.

The numerical studies of particle erosion are always helped by commercial Computational Fluid Dynamics (CFD) software [1-4], but some lasted achievements and complicated models are not included because of the lag of software development and the requirement to raise the calculation efficiency. For example, in Fluent, the squeeze film effect is not considered in particle-wall interaction model. Squeeze film is the liquid layer which has a cushioning effect on approaching particles. Clark [7] makes a quantitative analysis of the squeeze film in slurry erosion, results indicate that when the effect of the squeeze film is ignored, the erosion rate calculated value has a significant discrepancy with experiment, especially for small particles. Besides, the anisotropy of turbulence fluctuation that is important to particle dispersion calculation [8] are also absent.

In present work, a particle erosion prediction model is built to predict the worn profile of hydraulic spool valve. In this model, the flow flied is solved by Reynolds stress model, and other equations include particle trajectory model and particle erosion model are built and calculated by a self-made program. The program is more flexible than commercial CFD software, the squeeze film and detailed particle dispersion model are included, and the particle trajectory information can be obtained easily. Besides, the worn profile is generated by a time-discrete and spatial-discrete update method. The theoretical analysis is verified by laboratory experiments and a field case.

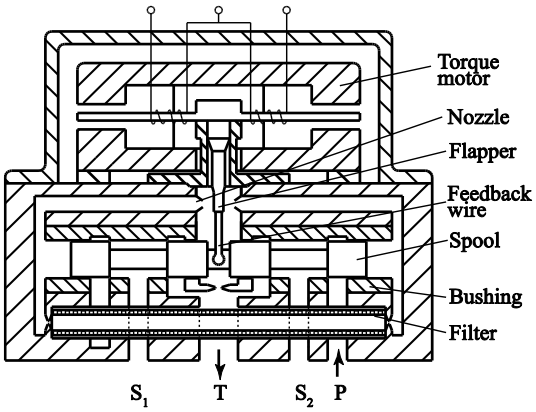

FIGURE 1. Structure Sketch of Servo Valve.

(Torque motor output a torque that proportional to the input current, causes a displacement of the flapper, leads to the change of the two jet nozzles throttle area, and finally produces a differential pressure on both ends of the spool. The spool displacement from null position leads to a feedback force on flapper through the feedback wire. Finally, the spool will stop at a force-balance position, and output a certain flow rate. Filter is used to protect the nozzle from blocking, and the fluid flow to spool bypasses the filter. P is supply port, S_1 and S_2 are service ports, and T is return port.)

1. THEORY AND MATHEMATICAL MODELING

The particle erosion prediction model of hydraulic spool valve can be divided into three parts:
1) Fluid phase model, obtaining the flow information by solving the Navier-Stokes equations.
2) Particle trajectory model, describing the trajectory of particle in turbulence flow and getting the vital information of impact velocity, impact angle and impact number as particles impact the target surface.
3) Particle erosion model, describing the mass loss of material as a particle impact the target surface with given velocity and impact angle.

1.1 Fluid Phase Model

The Navier–Stokes equations describe the motion of viscous fluid substances and reflect the basic mechanics of real flow. But the solving of N-S equations is very difficult and complicated because of its non-linear partial differential form. The approximate solution of turbulence flow can be obtained by solving the Reynolds averaged or space averaged N-S equations. Most turbulence models like viscous vortex model and large eddy simulation method are based on the assumption that the velocity fluctuation is isotropy, this assumption is appropriate for solving average flow field. But, for particles in turbulence, velocity fluctuation is the determining factor of theirs distribution propriety, and, unfortunately, the velocity fluctuation are anisotropy for almost all practical flow field [9]. Reynolds stress model (RSM) is a Reynolds averaged method where the Reynolds stresses is regarded as anisotropy and the variance of velocity fluctuation at different directions can be solved respectively. RSM approach originates from the work by Launder [9] Transport equation of Reynolds stresses in RSM can be expressed as

$$\frac{\partial}{\partial t}\left(\rho_f \overline{u_{f;i}u_{f;j}}\right)+\frac{\partial}{\partial x_{f;k}}\left(\rho_f \overline{U_{f;k}}\,\overline{u_{f;i}u_{f;j}}\right)=P_{ij}+D_{ij}+\Pi_{ij}-\varepsilon_{ij} \qquad \text{i)}$$

where, ρ_f is the density of fluid, μ is the dynamic viscosity of fluid, $\overline{U_f}$ is the temporal mean value of fluid velocity, u_f is the fluctuating velocity, $\rho\overline{u_{f;i}u_{f;j}}$ is the Reynolds stress, P_{ij} is the generation term of Reynolds stress, D_{ij} is the diffusion term, ε_{ij} is the destruction term, Π_{ij} is the pressure-strain term.

1.2 Particle Trajectory Model

1.2.1 Particle motion model

The motion of solid particle can be expressed as

$$m_p \frac{dU_{p;i}}{dt} = F_{D;i} + F_{G;i} + F_{P;i} + F_{L;i} + F_{VM;i} \qquad (1)$$

where, m_p is the particle mass, U_p is the particle velocity, F_D is the steady drug force, F_G are the forces due to gravity, F_P is the pressure-gradient force, F_L is the lift force , F_{VM} is the virtual mass force.
Stead drug force is the most important forces on particle motion and can be expressed as

$$F_{D;i}=\frac{18}{24}C_D m_p \frac{\mu \mathrm{Re}_p}{\rho_p d_p^2}\left(U_{pf;i}-U_{p;i}\right) \tag{2}$$

where, C_D is the drag coefficient which introduced in detail by Clift [10], d_p is the particle diameter, U_{pf} is the instantaneous fluid velocity at the particle location, Re_p is the relative Reynolds number.

$$\mathrm{Re}_p=\frac{\rho_f d_p}{\mu}\left|\overrightarrow{U_{pf}}-\overrightarrow{U_p}\right| \tag{3}$$

Buoyancy and the body force due to gravitation are calculated by

$$F_{G;i}=m_p g_i\left|1-\frac{\rho_f}{\rho_p}\right| \tag{5}$$

where, ρ_p is the particle density, g is the gravitational acceleration component. And pressure-gradient force is

$$F_{P;i}=m_p\frac{\rho_f}{\rho_p}\frac{\partial P}{\partial x_i} \tag{6}$$

The virtual mass force F_{VM} in Eq.(2) is only important for large particles (d_p>250 μm) [11] that are infrequent in hydraulic servo system. And the lift force is always very small and can be ignored [12].

1.2.2 Turbulent particle dispersion model

The discrete phase calculation is performed in a separate time step by Lagrange particle dispersion model. The time interval Δt is introduced to solve the motion of particles

$$U_{p;i}(t)=a_{p;i}+U_{p;i}(t-\Delta t)\Delta t \quad , \quad x_{p;i}(t)=x_{p;i}(t-\Delta t)+\frac{\Delta t}{2}\left[U_{p;i}(t)+U_{p;i}(t-\Delta t)\right] \tag{7}$$

where, a_p is the particle acceleration calculates by Eq. (2), $U_p(t)$, $x_p(t)$ are the velocity and location of particle on time t.

The pressure, instantaneous fluid velocity and Reynolds stresses are assumed to be constant over the small steps Δt. The time interval suggested by Gosman and Ioannides [13] is the minimum of either the turbulent eddy lifetime or the transit time taken for the particle to cross the eddy and pass from it

$$\Delta t=\min\left(\tau_{fL},\frac{l_e}{\left|U_f-U_p\right|}\right) \quad , \quad \tau_{fL}=A\frac{k}{\varepsilon} \quad , \quad l_e=B\frac{k^{1.5}}{\varepsilon} \tag{8}$$

where, l_e is the Kolmogorov length scale and τ_{fL} is the corresponding eddy lifetime by the Kolmogorov time scale. Constant A ranges from 0.135 to 0.41 in literatures [14], and B is determined by $B=A/\sqrt{1.5}$.

The instantaneous fluid velocity U_f which is required in particle equation of motion is given by

$$U_{pf;i}=\overline{U_{pf;i}}+u_{pf;i} \tag{9}$$

where, $\overline{U_{pf}}$ is the temporal mean velocity of fluid at the particle location, u_{pf} is the fluctuating fluid velocity at particle location that regarded as random variable because of the randomness of turbulence eddy.

The probability density function (PDF) of fluctuating fluid velocity is assumption to be Gaussian, and the mean of fluctuating fluid velocity is zero, the variance at specific location can be obtain by dividing the Reynolds stress by fluid density

$$P\left(u_{f;i}\right)=\frac{1}{\sqrt{2\pi}\sqrt{\overline{u_{f;i}^2}}}\exp\left[-\frac{u_{f;i}}{2\overline{u_{f;i}^2}}\right] \tag{10}$$

2.2.3 Particle-wall interaction model

The solid particle impact and rebound behavior in air is studied a lot by experiments, in which the Forder's model [15] based on tests using AISI4130 carbon steel as target is usually used in the plastic material erosion prediction. And Forder's model is given by

$$\begin{aligned} U'_{p;n}&=U_{p;n}e_n \quad , \quad e_n=0.988-0.78\alpha+0.19\alpha^2-0.024\alpha^3+0.027\alpha^4 \\ U'_{p;t}&=U_{p;t}e_t \quad , \quad e_t=1-0.78\alpha+0.84\alpha^2-0.21\alpha^3+0.028\alpha^4-0.022\alpha^5 \end{aligned} \tag{11}$$

where, $U'_{p;n}$ and $U'_{p;t}$ are the normal and tangential components of particle velocity after impact, $U_{p;n}$ and $U_{p;t}$ are the normal and tangential components of particle velocity before impact, α is impacting angle (the angle between the particle velocity vector and the target surface tangent vector).

For liquid-medium (petroleum hydraulic oil in present cases) and small-size-particle cases (almost particles diameter <30μm in present cases), the squeeze film effect is very important for erosion predict. In Clark's

research [7], squeeze film is defined as the thin layer of liquid separating approaching solid surfaces and which resist the close approach of those surfaces by their presence. The squeeze film factor F (the ratio of impact velocity normal component $U_{pimp;n}$ to approaching velocity normal component $U_{pa;n}$) was expressed in the relationship

$$F=\frac{U_{pimp;n}}{U_{pa;n}}=\max\left(\frac{a}{a+\xi}-\frac{12\xi^2}{a+\xi}\frac{1}{Re},0\right) \quad , \quad a=8\left(2\frac{\rho_p}{\rho_f}+f_{av}\right) \quad , \quad Re=\frac{\rho_f d_p}{\mu}U_p \tag{12}$$

where, Re is the Reynolds number of particle. And the values of ξ and f_{av} are discussed in detail in [15], according to the experiment of Clark (glass particle and water-medium which has the similar density ratio to the case in this paper), the ξ=13.1 and f_{av}=3.88 can be obtained.

1.3 Equations of Solid Particle Erosion

The erosion rate which defined as the mass of removed material due to unit mass particles impacting is the function of impact velocity, impact angle, particle properties, target material properties and environment variables. The erosion model summarized by Forder [15] is examined and used a lot

$$W=W_c+W_d \quad , \quad W_c=\frac{100}{2\sqrt{29}}\frac{3}{4\pi\rho_p}\left(\frac{U_p}{C_k}\right)^n\sin(2\alpha)\sqrt{\sin\alpha} \quad , \quad W_d=\frac{\left(U_p\sin\alpha-D_k\right)^2}{2E_f} \tag{13}$$

where, W_c is the erosion rate due to cutting action, W_d is the erosion rate due to deformation action. C_k and D_k are given by

$$C_k=\sqrt{\frac{3Y_f R_f^{0.6}}{\rho_p}} \quad , \quad D_k=\frac{\pi^2}{2\sqrt{10}}(1.59Y)^{2.5}\left(\frac{R_f}{\rho_t}\right)^{0.5}\left(\frac{1-q_p^2}{E_p}+\frac{1-q_t^2}{E_t}\right)^2 \tag{14}$$

The properties of particle and target material needed in Eq. (13) and (14) are listed in Table 1. The material of hydraulic spool valve, specifically the servo spool valve, is always high strength martensitic stainless steel (such as 440C). Quartz (SiO_2) is one of the common contaminants in hydraulic systems, and is selected in Vaughan's laboratory experiments [6]. Quartz particles are more regular in shape and closer to circularity than other common particles (such as SiC and $A1_2O_3$), and the erosion rate of quartz is much less according to the Bahadur's experiments [16]. So the quartz particle is assumed as sphere in this paper and the roundness factor of particle R_f is 1.

Besides, some empirical parameters needed in erosion model are also listed in Table 2. The erosion properties of stainless steel (include austenite, ferrite and martensitic stainless steel) is studied by Oka [17], and the velocity ratio exponent is expressed as the function of target material hardness Hv, particularly, n=2.3(Hv)$^{0.038}$ (Hv in units of GPa) for SiO_2 particle erosion. Besides, Arabnejad [18] obtain the velocity exponent of SS316 austenite stainless steel under quartz particle impact. The deformation erosion factor E_f of martensitic precipitation hardened stainless steel (17-4 PH) and structural steel (4130) is obtain from the research of Forder [15]. The composition and metallographic structure of 440C are more close to 17-4 PH (both of them belong to martensitic stainless steel), and the deformation erosion factor of 440C stainless steel in present model is 34 J/mm^3 proximately.

TABLE 1. Properties of particle and target material.

	Parameters		Unit	Value
Spool and Bushing (440C Stainless Steel)	Y_f	Plastic flow stress	MPa	760
	Y	Yield stress	MPa	450
	ρ_t	Density	kg/m^3	7650
	E_t	Young's modulus	GPa	200
	q_t	Poisson's ratio	-	0.28
	Hv	Surface hardness	GPa	5.8-6.2
Quartz Particle (SiO_2)	ρ_p	Density	kg/m^3	2650
	E_p	Young's modulus	GPa	59
	q_p	Poisson's ratio	-	0.23
	R_f	Roundness factor	-	1

TABLE 2. Empirical Parameters of Erosion Models

Parameters		Unit	Value	Notes
n	Velocity ratio exponent	-	2.3(Hv)$^{0.038}$	Oka[17]
			2.41	Arabnejad [18]
E_f	Deformation erosion factor	J/mm^3	34	17-4 PH(Forder [15])
			19	4130(Forder [15])

2. NUMERICAL PROCEDURE AND VALIDATION

2.1 Case Study

A four-passage zero-lap hydraulic spool valve is shown in FIGURE 2. There are four metering edges (A_1, B_1, A_2, B_2) in this valve. And these four metering edges can be divided into two types based on the flow direction: the direction of A_1 and B_2 is from tubing into spool cavity (P→S), and, A_2 and B_1 is from spool cavity to tubing (S→T).

We get two erosion cases of above hydraulic spool valve. Case 1 is the laboratory experiment performed by Vaughan et al. [6], worn profile and erosion mass loss are measurement accurately by specific instruments. In case 1, the detailed particle mass concentration (include the test start count and 48h test finish count) which is helpful to a more accurate calculation is given in TABLE 3. And according to Fitch's research [19], the particle mass concentration changes with time by exponential law. So, based on Table.3, the particle mass concentration during the course of tests can be calculated. Besides, the kinematic viscosity of oil is 15cSt at 60℃ and density is 863kg/m^3.

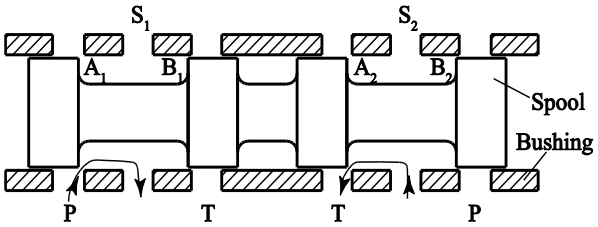

FIGURE 2. Four-Passage Zero-Lap Hydraulic Spool Valve (with a left displacement of spool)

TABLE 3. Particle Mass Concentration
(For case 1, 48h test, at 7MPa differential pressure)

Rang /μm	Median size/ μm	Uncut quartz/ mg Ł$^{-1}$		0-10um cut/ mg Ł$^{-1}$	
		Start	Finish	Start	Finish
<2.5	1.25	3.61	3.61	5.64	8.39
2.5-7.5	5	3.20	2.42	3.44	3.29
7.5-12.5	10	0.503	0.322	0.353	0.191
12.5-17.5	15	0.0886	0.0494	0.0553	0.0217
17.5-22.5	20	0.0262	0.0130	0	0
>22.5	25	0.00955	0.00437	0	0
SUM		7.44	6.42	9.49	11.9

Case 2 is a field case, the match grinding curve of a jet pipe servo valve is measurement before and after the 200h life test respectively to evaluate the wear loss of spool valve metering edge. The photo of the worn spool metering edge after the life test is shown in FIGURE 3. And the contamination level of the test system is 14/11 (ISO 4406), the main contamination is quartz particles. The oil used in case 2 is 10# aircraft hydraulic oil, and medium temperature is 60℃ approximately. Besides, the life test of servo valve is done under 21MPa supply pressure, 0.6MPa oil return pressure and without load, so the differential pressure for each metering edge is 10.2MPa.

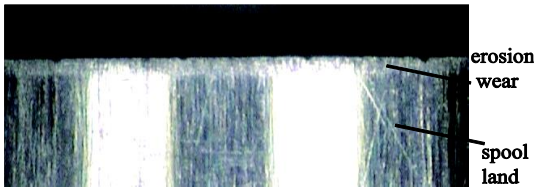

FIGURE 3. Photo of the Worn Spool Metering Edge after the Life Test (case 2)

2.2 Numerical Procedure and Method

As mentioned, the numerical model of solid particle erosion can be divided into three parts. Among them, the fluid phase model is solved by the commercial CFD software, because the calculation method in CFD software is optimized and mature. Because the flow filed of spool valve is axisymmetric, instead of a 3-D model, the 2-D symmetry boundary conditions is selected to ensure a more efficient calculation.

But for particle trajectory model and erosion model, the commercial CFD software just provide some simplified

models (time and spatial correlation of turbulent eddy and Hashish's erosion equation are not included). Although the user define function (UDF) is supposed, the writing and solving of these functions is under the frame of the software and the acquirement of intermediate variables is not convenient. So, the equations of particle trajectory model and erosion model are built and solved under MATLAB environment. As FIGURE 4 shows, the particles information (include particle material property, diameter and number) and flow phase information solved by commercial CFD software are imported to MATLAB programs as input variables, then the particles motion are solved by the self-made programs.

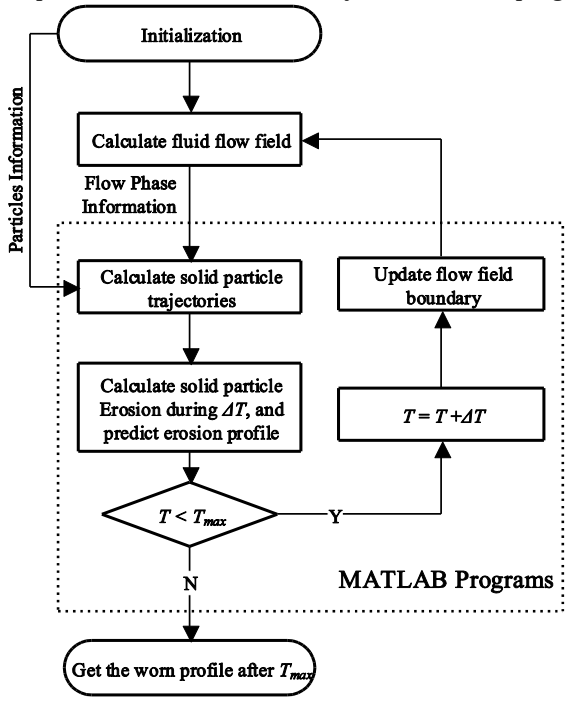

FIGURE 4. Flow Diagram of Numerical Procedure

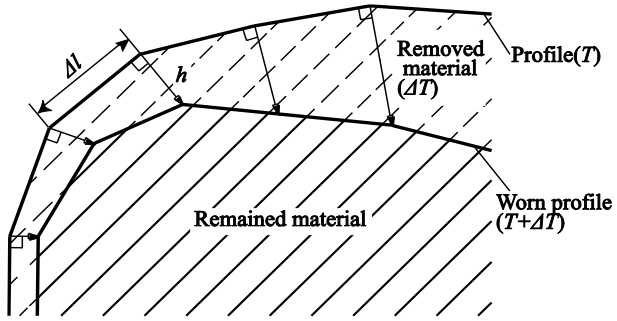

FIGURE 5. A Time-Discrete and Spatial-Discrete Update Method of Worn Profile

As FIGURE 5 shows, a time-discrete and spatial-discrete update method is proposed. The profile of spool and bushing is divided into several small parts (spatial-discrete, the length of each part Δl=5μm in present model), the removed material volume of each part during time-step ΔT (time-discrete) is given by

$$V(l)=\frac{\sum_{i=1}^{m} W_p(i)}{\rho_t} \tag{15}$$

where, m is the count of particles that impact the part Δl during time-step ΔT, $W_p(i)$ is the mass loss of target material due to the impact of particle i. And the endpoint of small part moves to inner alone the normal of surface to generate the new profile. The moving distance of endpoint is expressed as

$$h(l)=\frac{V(l)}{\pi D \Delta l} \tag{16}$$

Then, the fluid field is calculated again with the new boundary conditions.

3. RESULTS AND DISCUSSION

3.1 Shape of Worn Profile (Case 1)

First, the local erosion depth h_s (for spool) and h_b (for bushing) are selected as the quantitative description indexes of the metering edges profile. As FIGURE 6 shows, h_s and h_b are the function of l_s (the distance from the point at spool profile to spool land edge) and l_b (the distance from the point at bushing profile to bushing internal surface) respectively. For flow from spool cavity to tubing cases, the definition of l_s and l_b are the distance to spool land surface and the distance to bushing port edge respectively. And the total erosion loss can be described with the area between initial profile and worn profile. Besides, the opening x_{v0} is defined as the distance between the spool land edge and bushing port edge, and the actual width of

throttle area (x_v) is defended as the minimum distance between the profile of spool and bushing.

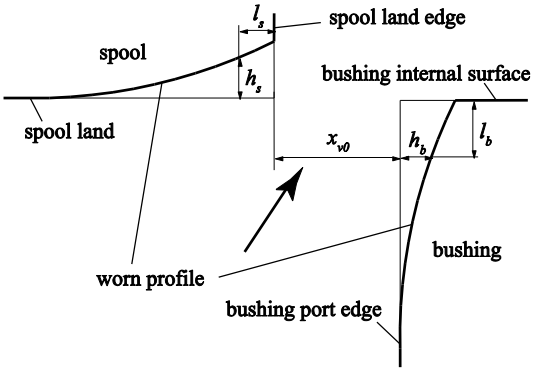

FIGURE 6. Quantitative Description of Worn Profile

Vaughan's experiments (case 1) give the profile of spool and bushing when the total wear loss of bushing W_b is 581μm^2 and 807μm^2. Numerical simulation worn profile is also calculated under the same conditions, and the termination condition of the numerical procedure in FIGURE 4 is modified to that the total wear loss of bushing is not less than the given value (581μm^2 and 807μm^2). The simulation and experiment worn profile under the same bushing wear loss are shown in FIGURE 7.

The theoretical shape of bushing worn profile accord well with the experimental results. Although the final spool wear loss of simulation (388μm^2) has a 9% disparity to experiment (356μm^2), the downstream (l_s<40μm) worn profile shape are also fitting well.

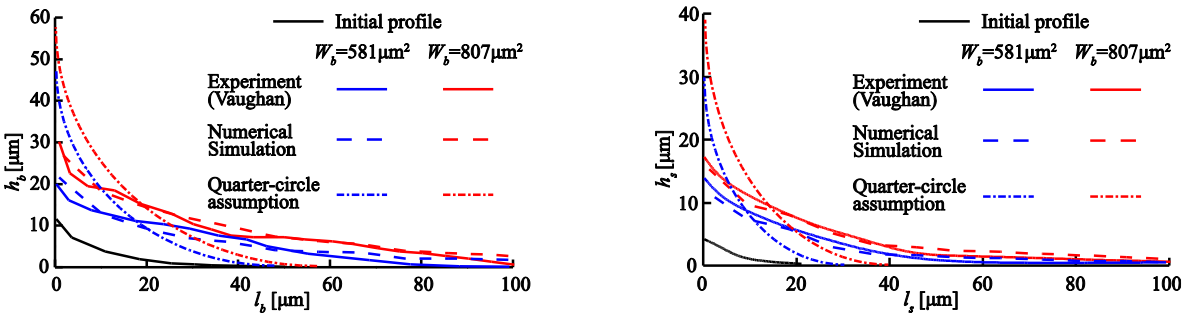

(a) (b)

FIGURE 7. Worn Profile under the Given Wear Loss of Bushing W_b (a) Bushing, (b) Spool.

When W_b=581μm^2, the corresponding wear loss of spool W_s of Vaughan's experiment is 222μm^2 and simulation result is 226μm^2. When W_b=803μm^2, W_s of Vaughan's experiment is 356μm^2 and simulation is 388μm^2. The profiles under the quarter-circle assumption are obtained based on the experiment wear volume.

In some studies [5], the worn profile of metering edge is always simply assumed as quarter-circle that tangent to the port edge and internal surface (for bushing). Then, the circle radius and the throttle area width x_v can be obtained by geometrical equations if the wear volume is given. The profiles of quarter-circle assumption are shown in FIGURE 7, obviously, the quarter-circle assumption are very different from the experiment and numerical simulation results. This difference can causes not only a different flow condition at metering edge, but also a large error of throttle area calculation. As TABLE.4 shows, the throttle area width x_v of quarter-circle assumption is incorrect, especially for null position, this will cause an erroneous result for null leakage calculation.

TABLE 4 The throttle area width x_v when the wear loss of bushing W_b=581μm^2.

	x_{v0}=0		x_{v0}=100μm	
	x_v [μm]	Error	x_v [μm]	Error
Vaughan's experiment	24.1	-	119	-
Numerical simulation	24.4	1.2%	120.8	1.5%
Quarter-circle assumption	44	82.6%	125.9	5.8%

3.2 Field Test (Case 2)

First, a quantitative evaluation method (match grinding curves) of the erosion is introduced.

Pneumatic match grinding curves that record the flow characteristics of each metering edge are always used to measurement the null lap of spool valve. The throttling process of air at metering edge is adiabatic

and isentropic, according to throttle equation, the air leakage has a liner relationship with the width of actual throttle area x_v. For the as-received new spool vale, the metering edge can be regarded as the quadrant which radius is r, and the width of actual throttle area x_v can be expressed as

$$x_v = \sqrt{(x_{v0}+2r)^2+(b+2r)^2}-2r \tag{17}$$

where b is the radial clearance between spool and bushing. And for the worn metering edge, the x_v is the distance between the corner of spool and bushing

$$\begin{cases} x_v = \sqrt{(x_{v0}+h_{b0})^2+(b+h_{s0})^2} & \text{P}\rightarrow\text{S} \\ x_v = \sqrt{(x_{v0}+h_{s0})^2+(b+h_{b0})^2} & \text{S}\rightarrow\text{T} \end{cases} \tag{18}$$

Both for Equ.(17) and (18), when the opening x_{v0} is large enough, the r, b, h_{s0} and h_{b0} can be ignored, and the relation between x_v and x_{v0} is approximate linear. So the match grinding curves shown in FIGURE 8 have the linear region when the opening of spool valve is large, and the curves become nonlinear for small opening.

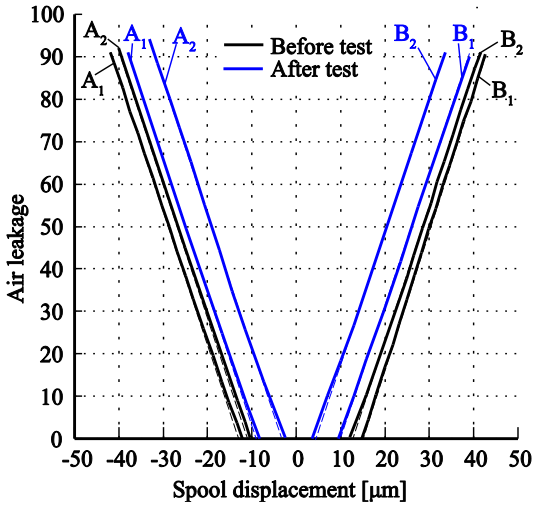

FIGURE.8 Match Grinding Curve Before and After the 200h Life Test.

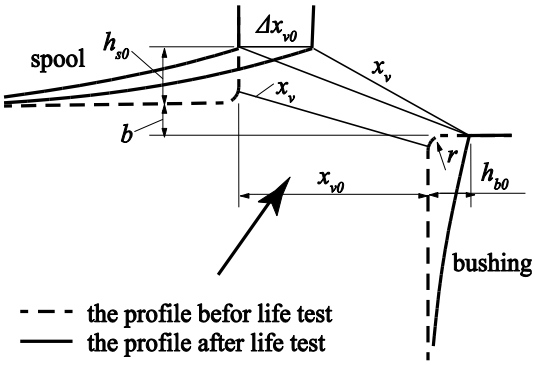

FIGURE 9 Schematic Diagram of Geometric Relationship. (Flow from tubing into spool cavity)

The match grinding curves before and after life test are shown in FIGURE 8. The linear region slope of the curves are almost unaltered with the erosion, this means the flow coefficient can be regarded as constant. So the erosion just causes the horizontal translation of match grinding curves, and the erosion can be evaluated quantitatively by the translation displacement Δx_{v0}. As shown in FIGURE 9, the physical significance of Δx_{v0} is the opening difference between the new as-received and worn spool valve when their air leakage are the same.

After getting the experimental curves shown in FIGURE 8, the experimental translation displacement Δx_{v0} can be obtained by drawing a horizontal straight lines that has intersections with the linear region of the curves (Air leakage=80 is selected to meeting the criteria), and the distance between the intersections on before-test and after-test curves is what we want.

For theoretical calculation, according to the geometric relationship in FIGURE 9, the theoretical opening difference Δx_{v0} can be calculated by

$$\Delta x_{v0} = h_{b0} + x_{v0} - \sqrt{x_v^2-(b+h_{s0})^2} \tag{19}$$

The numerical simulation is done based on the conditions in section 2.1 (case 2). The field test and simulation results shown in Table.5 indicate that the erosion of S→T direction is more serious. The field test and simulation results agree well.

TABLE 5. The Opening Difference Δx_{v0} of Field Test and Simulation (case 2)

Direction	Metering edge	Field test/μm	Simulation/μm
P→S	A_1	3.6	3.96
	B_1	3.8	
S→T	A_2	7.9	7.35
	B_2	7.9	

5. Conclusion

1) In the present work, a numerical mechanism model is presented in detail to predict the solid particle erosion in hydraulic spool valve. First, the fluid phase is solved by Reynolds stress model (RSM) to consider the anisotropy of turbulence velocity fluctuation. Second, a stochastic separated flow (SSF) model based on eddy interaction is established to obtain the particle trajectory. Third, the local erosion rate is calculated by erosion formula. Then, based on the local erosion rate, a time-discrete and spatial-discrete method is proposed to obtain and update the worn profile. The fluid phase model is solved in commercial CFD software, and the other models are established and solved by self-made program. This numerical method of solid particle erosion can be used not only in spool valve but also the other hydraulic component.
2) The worn profile are studied through the numerical model. The results of simulation and Vaughan's experiment indicate that, the metering edge worn profile is not quarter-circle, and an erroneous erosion prediction may be caused under the quarter-circle assumption.
3) Laboratory experiments and a field test are selected to verify the validity of the model. The horizontal translation of match grinding curves are used to evaluate the erosion quantitatively. The field test results and the model results agree well, and the present model is practicable for solid particle erosion of spool valve.

ACKNOWLEDGMENTS

This work is supported by the National Natural Science Foundation of China (Grant no. 51475332).

REFERENCES

1. Grant G, Tabakoff W. Erosion prediction in turbomachinery resulting from environmental solid particles [J]. Journal of Aircraft, 1975, 12(5): 471-478.
2. Zhong Y, Minemura K. Measurement of erosion due to particle impingement and numerical prediction of wear in pump casing[J]. Wear, 1996, 199(1): 36-44.
3. Njobuenwu D O, Fairweather M. Modelling of pipe bend erosion by dilute particle suspensions[J]. Computers & Chemical Engineering, 2012, 42: 235-247.
4. Wallace M S, Dempster W M, Scanlon T, et al. Prediction of impact erosion in valve geometries[J]. Wear, 2004, 256(9): 927-936.
5. Fang X, Yao J, Yin X, et al. Physics-of-failure models of erosion wear in electrohydraulic servovalve, and erosion wear life prediction method [J]. Mechatronics, 2013, 23(8): 1202-1214.
6. Vaughan N D, Pomeroy P E, Tilley D G. The contribution of erosive wear to the performance degradation of sliding spool servovalves [J]. Proceedings of the Institution of Mechanical Engineers, Part J: Journal of Engineering Tribology, 1998, 212(6): 437-451.
7. Clark H M I. The influence of the squeeze film in slurry erosion[J]. Wear, 2004, 256(9): 918-926.
8. Balachandar S, Eaton J K. Turbulent dispersed multiphase flow[J]. Annual Review of Fluid Mechanics, 2010, 42: 111-133.
9. Launder B E, Reece G J, Rodi W. Progress in the development of a Reynolds-stress turbulence closure[J]. Journal of fluid mechanics, 1975, 68(03): 537-566.
10. Clift R, Grace J R, Weber M E. Bubbles, drops, and particles[M]. Courier Corporation, 2005.
11. Meng H, Van der Geld C W M. Particle trajectory computations in steady non-uniform liquid flows[J]. ASME, Fluids Engineering Division (Publication) FED, 1991, 118: 183-193.
12. Mei R. An approximate expression for the shear lift force on a spherical particle at finite Reynolds number[J]. International Journal of Multiphase Flow, 1992, 18(1): 145-147.
13. Isaac B J, Parente A, Galletti C, et al. A novel methodology for chemical time scale evaluation with detailed chemical reaction kinetics[J]. Energy & fuels, 2013, 27(4): 2255-2265.
14. Savva N, Kalliadasis S, Pavliotis G A. Two-dimensional droplet spreading over random topographical substrates[J]. Physical review letters, 2010, 104(8): 084501.
15. Forder A, Thew M, Harrison D. A numerical investigation of solid particle erosion experienced within oilfield control valves[J]. Wear, 1998, 216(2): 184-193.
16. Bahadur S, Badruddin R. Erodent particle characterization and the effect of particle size and shape on erosion[J]. Wear, 1990, 138(1-2): 189-208.
17. Oka Y I, Yoshida T. Practical estimation of erosion damage caused by solid particle impact: Part 2: Mechanical properties of materials directly associated with erosion damage[J]. Wear, 2005, 259(1): 102-109.
18. Arabnejad H, Mansouri A, Shirazi S A, et al. Development of mechanistic erosion equation for solid particles[J]. Wear, 2015, 332: 1044-1050.
19 Fitch E C. Hydraulic component design and selection[M]. Bardyne. Incorporated, 2004.

